Article

Korean Amberjack Skin-Inspired Hyaluronic Acid Bioink for Reconstruction of Human Skin

Hoai-Thuong Duc Bui, Wanho Cho, Jae Keun Park, Moon Sue Lee, Hong Kee Kim, and Hyuk Sang Yoo*

Read Online

ACCESS | Metrics & More | Article Recommendations | Supporting Information

ABSTRACT: Decellularized extracellular matrix (dECM) has been extensively employed as tissue engineering scaffolds because its components can greatly enhance the migration and proliferation of cultivating cells. In this study, we decellularized Korean amberjack skin and incorporated soluble fractions in hyaluronic acid hydrogels with 3D-printed tissue engineering hydrogels to overcome any limitation of animal-derived dECM. The hydrolyzed fish-dECM was mixed with methacrylated hyaluronic acid and chemically crosslinked to 3D-printed fish-dECM hydrogels, where fish-dECM contents affected both printability and injectability of the hydrogels. Swelling ratios and mass erosion of the 3D-printed hydrogels were dependent on fish-dECM contents, where higher

fish-dECM in the hydrogel increased swelling ratios and mass erosion rates. The higher content of fish-dECM considerably enhanced the viability of the incorporated cells in the matrix for 7 days. Artificial human skin was constructed by seeding human dermal fibroblasts and keratinocytes in the 3D-printed hydrogels, and a formation of a bilayered skin was visualized with tissue staining. Thus, we envision that 3D-printed hydrogels containing fish-dECM can be an alternative bioink composed of a non-mammal-derived matrix.
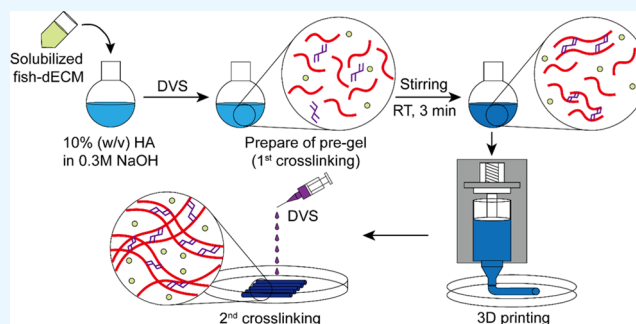
1. INTRODUCTION

The hyaluronic acid (HA)-based three-dimensional (3D) printing system has gained attention in the field of tissue engineering owing to its flexibility to design and fabricate 3D structures or artificial tissues with high stability, nonimmunogenic nature, and good biocompatibility, which may enhance cell behavior.[1] HA is a natural glycosaminoglycan (GAG) found in almost all tissues and organs. It has a vital role in promoting the reconstruction, proliferation, and migration of fibroblasts and endothelial cells, and is also involved in angiogenesis.[2,3] HA improves the shear-thinning and extrusion properties of 3D printing, which supports the feasibility of the bioink.[4,5] However, unmodified and pure HA is rarely employed for 3D printing because of its unstable viscosity to maintain a 3D structure.[3,6] Thus, many researchers have chemically modified HA or mixed this material with a printable polymer (e.g., alginate or gelatin) for 3D printing.[6−8] Nevertheless, chemical modification of HA is a complex process and usually requires a long reaction time. Additionally, manipulating the gelation process is essential to maintain the 3D structure of the HA scaffold after the printing process. Many chemical crosslinking methods have been studied for the gelation of HA molecules such as 1-ethyl-3-(3-dimethylaminopropyl) carbodiimide (EDC), ethylene glycol diglycidyl ether (EX-810), glutaraldehyde (GA), and 1,4-butanediol

diglycidyl ether (BDDE).[9−12] Divinyl sulfone (DVS), which can react with the hydroxyl group of HA at a high pH and room temperature to produce sulfonyl bis-ethyl links, has been widely used as a crosslinking compound for HA gelation because it can shorten the reaction time compared to other chemical crosslinking agents.[12]

The decellularized extracellular matrix (dECM) has been used as a biocompatible material in various forms, such as injectable hydrogels,[13−15] dermal hydrogels, sheet, and powder,[16,17] in tissue engineering for supporting the regeneration of skin,[18,19] cartilage,[20,21] and blood vessels.[14,22] dECM maintains the main extracellular matrix structures and biochemical components of the original tissue or organ, including collagen, GAGs, and growth factors, which can enhance cell behaviors, while eliminating the cellular material and DNA content to avoid immune responses.[23] Mammalian-derived dECM, especially dECM from cattle and pig, has attracted extensive research in recent decades, and has been
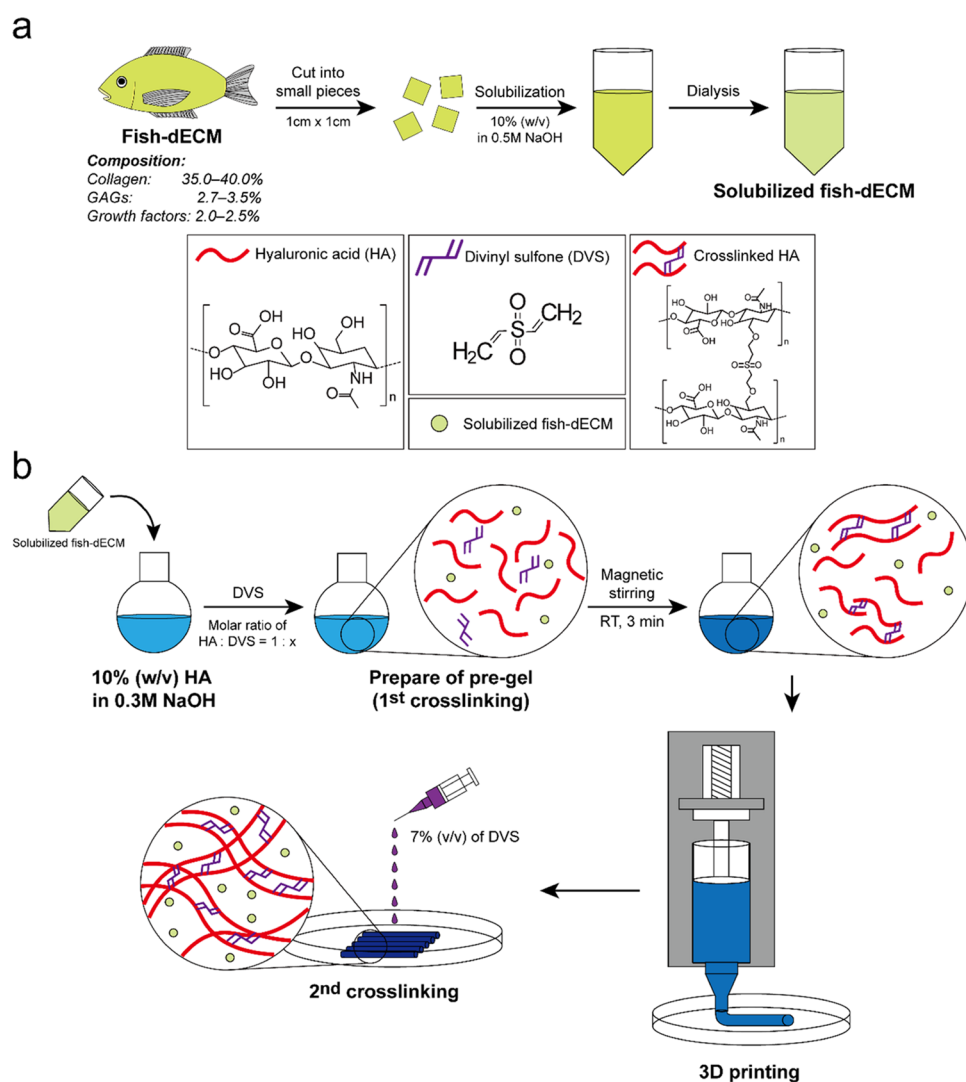
Figure 1. Schematic diagram of the preparation of solubilized fish-dECM and 3D hybrid bioink for cocultivation of HDF and HaCaT cells with a 3D-printed model in an air−liquid condition. (a) Solubilization process of fish-dECM in alkaline conditions. (b) Preparation of 3D hybrid bioink (pre-gel) and fabrication of a 3D-printed model via 3D printing and secondary crosslinking of the 3D scaffold.

utilized in most of the commercially available bio-scaffolds such as Durepair, Pelvicol, Permacol, PriMatrix, and SurgiMend.[17] However, because of the risk of infectious diseases such as bovine spongiform encyclopedia (BSE),[2] transmissible spongiform encephalopathy (TSE), avian and swine influenza, and foot-and-mouth disease (FMD) from mammalian-derived dECM, numerous questions have been raised as to whether this material should be continued widely using in human clinical applications.[24] Moreover, immunogenicity, high cost of fabrication, and religious limitations have been considered additional drawbacks, which stimulate many researchers to find better alternatives. Fish-derived dECM has been found to contain similar composition compared to mammalian-derived dECM including collagen, GAGs, and several growth factors that positively affect wound healing,[2,25] while causing a relatively lower immune response than mammalian-originated materials. A study on the high biocompatibility of collagen-based 3D structures extracted from fish-derived decellularized skin highlighted the feasibility of the same in tissue engineering.[26] In addition, a biocompatible hydrogel from fish-derived decellularized skin-extracted collagen was successfully prepared, which generated

the formation of epidermal layers and maturation of skin appendages, and thus, accelerated wound healing compared to commercial products.[2] Most previous studies were conducted on fish collagen-based hydrogel for skin regeneration since collagen was proved to support the growth, proliferation, attachment, and infiltration of fibroblasts and keratinocytes.[2,24,27,28] Nevertheless, single components such as collagen do not provide a natural enriched composition of the skin dermis that could simulate an appropriate biological and biomechanical environment in which fibroblasts function. It has been proved that the matrix with full-thickness skin-dECM brought better mechanical properties and also improved cell behavior compared to pure collagen matrix due to the rich microenvironment, which induced better fibroblast interaction.[29]

In the current study, we proposed an HA-based hybrid ink composed of a solubilized decellularized fish skin matrix and HA at different weight ratios. The mixture was further crosslinked with DVS at a low molar ratio to obtain a pre-gel of the hybrid ink with stable viscosity for 3D printing. The 3D-printing process of custom-designed models was performed using the pre-gel and followed by secondary crosslinking with

Table 1. Characterization of the Weight of Solubilized Fish-dECM, and Total Protein Performed by the BCA Assay Depending on Solubilized Time

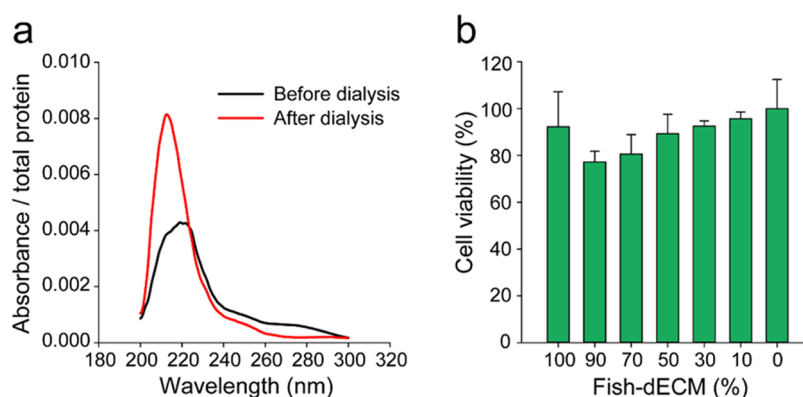| fish-dECM solubilization time (hours)	initial weight of fish-dECM (mg)	unsolubilized fish-dECM (mg)	solubilized fish-dECM (mg)[a]	total protein (μg/mL)	
				before dialysis	after dialysis
4	1000	30.7 ± 5.6	211.4 ± 6.8	741.1 ± 34.0	116.2 ± 1.4
12		32.0 ± 2.5	291.7 ± 9.6	434.7 ± 87.9	157.7 ± 2.5
24		12.2 ± 1.4	182.3 ± 6.5	305.6 ± 43.2	172.0 ± 3.7
48		11.1 ± 1.3	73.8 ± 14.7	246.7 ± 51.8	136.8 ± 3.6

[a]Weight of solubilized fish-dECM after dialysis.

Figure 2. Characterization of dECM. (a) UV−vis spectra of solubilized fish-dECM before or after dialysis. Absorbance was normalized to total protein determined by a BCA assay. (b) Cytotoxicity of fish-dECM eluant. Fish-dECM (6 cm²) was eluted with DMEM supplemented with 10% of FBS (1 mL), followed by mixing with cell cultivation medium at different mixing ratios (0−100%) and addition to NIH3T3 cells (1 × 10⁴ cells/well (surface area = 0.32 cm²)). After 24 h, an MTT-based cytotoxicity assay was performed and the viability of the treated cells was normalized with respect to those without treatment.

higher DVS concentration to maintain the 3D structure of the scaffold. Studies on decellularized matrices have shown that the decellularized matrix contains collagen, GAGs, and several growth factors and may support cell adhesion, migration, and differentiation because it maintains the characteristics of the ECM structure of tissue/organ.[23,30] Therefore, we hypothesize that our HA-based hybrid scaffold can be used to regulate cell adhesion, migration, and proliferation.[11]

2. RESULTS AND DISCUSSION

Fish-derived decellularized skin has several water-soluble proteins such as collagen, GAGs, and growth factors, which have advantageous effects on wound healing and cell growth.[31] While collagen was proved to enhance the growth, proliferation, attachment, and infiltration of fibroblasts and keratinocytes, which support skin generation and wound healing,[28] a previous study demonstrated that growth factors and GAGs had a correlation with in vivo constructive remodeling of biological scaffolds.[31,32] Therefore, it is necessary to extract these cell-friendly factors for further incorporation in the hybrid ink. However, because of their strong attachment to the substrate by peptide bonds, many researchers treated fish-derived decellularized skin in acid or basic conditions.[2,25,27,33] Besides, collagens are almost insoluble in alkali solution while noncollagenous proteins are the opposite, and also short-term alkaline pretreatment does not influence collagen biochemical properties. Thus, alkali solution has been used as a safe pretreatment strategy to remove noncollagenous proteins in collagen extraction.[27,33,34] Moreover, antigenicity is related to the presence of non-collagenous proteins;[35] hence, it is important to eliminate

these components to enhance the safety of dECM for clinical applications. Among different kinds of alkali solution, NaOH and Ca(OH)$_2$ were frequently used as they showed similar good ability to remove noncollagenous proteins while ensuring the minimal loss of collagen after the reaction.[33] Therefore, in our study, the decellularized fish-derived skin was solvated in NaOH solution for 4, 12, 24, and 48 h, and then, dialysis was performed to remove salts, impurities, and fragmented proteins in the solubilized product (Figure 1a). Total proteins before and after dialysis were analyzed by the BCA assay (Table 1). According to the BCA assay results, total proteins initially increased and then decreased upon prolonging the solubilization time. Particularly, after 4 h, the total protein before dialysis reached the highest at 741.1 ± 34.0 μg/mL, but after dialysis, it remarkably diminished to the lowest at 116.2 ± 1.4 μg/mL. This is because the noncollagenous proteins in the decellularized fish-derived skin were soluble in the early stage of the solvate process, and then removed through dialysis.[33,34] In the case of 12 and 24 h, the total proteins after dialysis were 157.7 ± 2.5 and 172.0 ± 3.7 μg/mL, respectively, thereby indicating that collagen and proteins in the decellularized fish-derived skin were sufficiently soluble. A previous study evaluated the effect of reaction time from 1 to 12 h, at NaOH concentration from 0.05 to 0.5 M, and temperature from 4 to 20 °C on the quantity of removed proteins; the quantity of removed proteins accelerated maximally as the reaction time was increased up to 12 h, concentration of NaOH reached up to 0.5 M, and the temperature raised up to 20 °C.[33] Similar results have been indicated by Woo et al.:[27] pretreatment periods from 12 to 36 h and NaOH concentration between 0.5 and 1.3 M gave the maximum
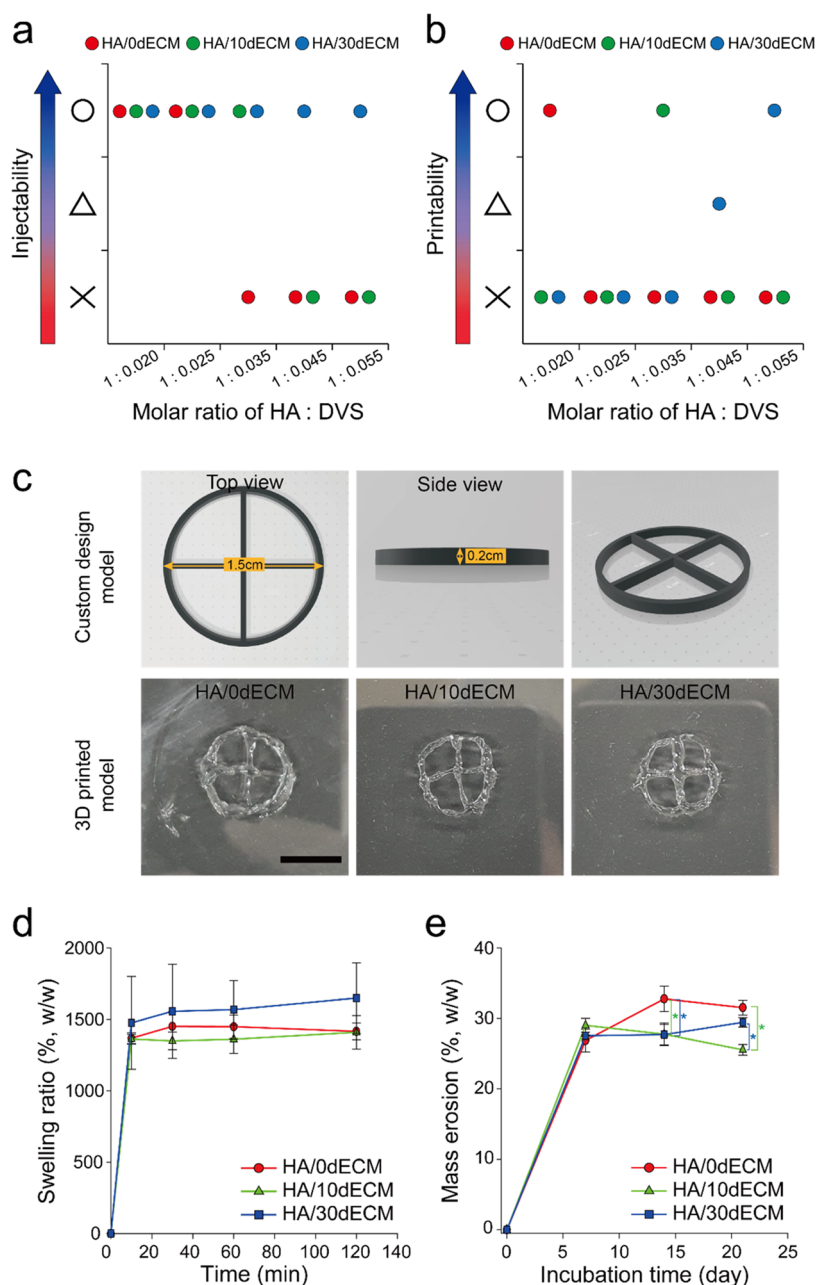
Figure 3. Investigation of injectability and printability of different HA-based bioinks, and characterization of 3D-printed models. (a, b) Optimization of 3D hybrid bioink. Injectability and printability of 3D hybrid bioink crosslinked at various DVS molar ratios (molar ratio of HA:DVS = 1:0.020−0.055) were examined (O, high; Δ, medium; X, low injectability/printability). (c) Images of the custom design model and 3D-printed model (scale bar = 1 cm). (d) Water swelling ratio of the 3D-printed model with 7% (v/v) DVS ($n = 3$). (e) Mass erosion of 3D-printed model; 3D-printed model was immersed in PBS (pH 7.4) at 37 °C for 7, 14, and 21 d. At the designated time point, the degraded 3D model was washed thrice with DW and freeze-dried; the dried 3D model weight was recorded ($n = 3$). *indicates a significant difference between HA/0dECM, HA/10dECM, and HA/30dECM; $p < 0.05$ were considered statistically significant.

collagen content extracted from yellowfin tuna skin. Total protein was found to reduce at 136.8 ± 3.6 μg/mL when we increased the reaction time up to 48 h. This could be due to the fragmentation of soluble proteins caused by the negative effect of NaOH. It has been reported that a longer duration of pretreatment with NaOH might cause a higher loss of proteins.[36] The results from other studies also revealed that peptide linkages were broken when treated with NaOH for a long time.[37,38] Therefore, a solubilization time of 12 h was utilized for further experiments in this study to optimize the effect of alkali solution in removing the noncollagenous

proteins without risking any negative influence of NaOH on the fish-dECM.

Proteins generally have maximum absorbance at 280 nm due to the presence of tryptophan. However, dECM primarily contains collagen, which is mostly composed of glycine, followed by proline and hydroxyproline; thus, the maximum absorbance should be in the range of 210−240 nm.[39,40] Herein, we analyzed the normalized absorbance (Figure S1) and the absorbance/total protein ratio (Figure 2a) of the solubilized decellularized fish-derived skin before and after dialysis. Both the normalized absorbance and the absorbance/
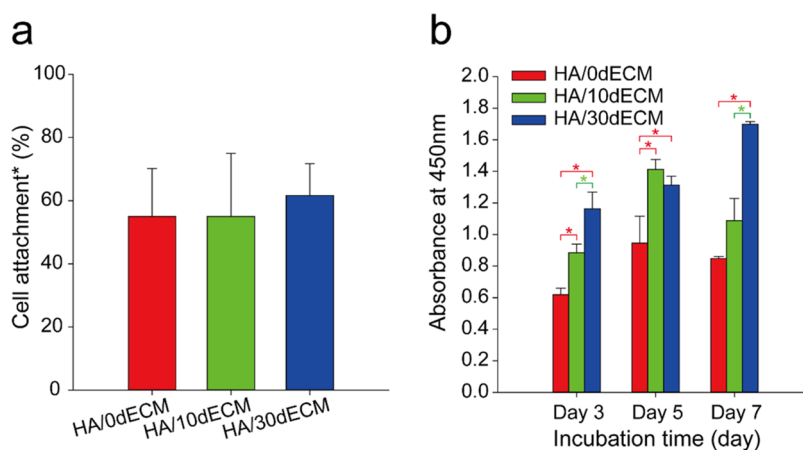
Figure 4. *In vitro* studies on cell attachment and cell viability of HA-based 3D-printed scaffolds. (a) NIH3T3 cells attachment on 3D-printed models. Unbound cells were stained with trypan blue and counted using a hemocytometer. Cell attachment* (%) = ((number of initial cells − counted cells)/number of initial cells × 100). (b) Proliferation of cells cultivated on 3D-printed models for 3, 5, and 7 d ($n = 3$). Cell proliferation was determined by a WST-1-based colorimetric assay. * indicates a significant difference between HA/0dECM, HA/10dECM, and HA/30dECM; $p < 0.05$ were considered statistically significant.

total protein ratio of the solubilized fish-dECM after dialysis were sharply augmented at the wavelength range of 210−240 nm compared to those before dialysis. This confirmed that most noncollagenous proteins were removed during dialysis, and the collagen in the solubilized fish-dECM became more concentrated after dialysis. The results also revealed that the use of short-term alkali pretreatment in our study did not lead to the denaturation of collagen, which was in accordance with previous studies in which proline and hydroxyproline were investigated to be broken only after treating with NaOH for several days.[37] Therefore, we supposed that our solubilization methods of fish-dECM successfully concentrated the required factors for skin regeneration and wound healing. Regarding the cytotoxicity test of fish-dECM on NIH3T3 cells based on the MTT assay (Figure 2b), there was no significant difference among groups of fish-dECM eluent treated cells compared to untreated cells. Especially, at 100% of fish-dECM eluent, the cell viability was shown to be similar to fish-dECM untreated cells, which meant that fish-dECM was biocompatible with cells. The results are in accordance with previous studies, in which C619 epithelial cells exhibited high viability when being treated with fish-dECM extracted from grass carp skin.[41]

Different dECM-combined HA-based hybrid inks—HA/0dECM, HA/10dECM, and HA/30dECM—were prepared by dissolving HA and dECM in 0.3 M NaOH solution and subsequently crosslinking using different molar ratios of DVS to form a pre-gel. The different bioinks were evaluated for their injectability, which allows them to be extruded constantly and homogeneously from the syringe, and printability, which relates to the shape fidelity of 3D-printed models. Because of the discrete change of different bioinks between "low" and "high", a qualitative assessment was conducted instead of quantitative analysis. Considering the high injectability and printability of different molar ratios of HA:DVS (Figure 3a,b) as well as the stable formation of the 3D-printed scaffold, molar ratios of 1:0.035 and 1:0.055 were chosen for initial crosslinking of HA/10dECM and HA/30dECM, respectively. Regarding HA/0dECM, although the molar ratio of HA:DVS at 1:0.020 gave the best injectability and printability, the postprinting shape of the model was not well maintained. Thus, we slightly increased the amount of the crosslinking

agent, and a molar ratio of 1:0.025 was employed for further experiments with HA/0dECM. After the 3D model was successfully printed using the modified HA-based hybrid ink, DVS (5, 7, and 10%; v/v) was additionally dropped on the printed model for secondary crosslinking (Figure 1b). The design model and 3D-printed scaffolds with different weight ratios of HA:dECM are shown in Figure 3c. The strategy of utilizing dual crosslinking in 3D printing has been employed by several researchers.[4,6,42] The initial crosslinking aims to optimize the injectability and printability as well as the shape fidelity of the bioink. Meanwhile, the later crosslinking is necessary to stabilize the shape of the 3D-printed scaffold. In the studies of Petta et al., horseradish peroxidase and hydrogen peroxide-mediated enzymatic crosslinking of tyramine functionalized HA was introduced as the first crosslinking method of the bioink, and eosin Y-induced photocrosslinking was secondarily applied on the 3D matrix to form a stable construct.[4]

The swelling property plays an important role in the circulation of nutrients, oxygen, and cell waste removal, as well as the absorption of exudates and body fluids secreted from wounds.[43] Therefore, the swelling ratio of the secondary crosslinked models with various concentrations of DVS was measured (Figures 3d and S2). There was no substantial difference in the swelling ratio of the secondary crosslinked models with 5 and 7% (v/v) of DVS, but in the case of the 3D scaffolds crosslinked with 10% (v/v) of DVS, the swelling ratio of the HA/30dECM-based model was the highest among the other two groups and was similar to the HA/30dECM-based models crosslinked with 5 and 7% (v/v) of DVS. This could be due to the least amount of HA presented in HA/30dECM, and 7% (v/v) of DVS was adequate for fully crosslinking of HA in HA/30dECM. Thus, an increase of the DVS ratio to 10% could not induce further crosslinking of HA/30dECM. In the cases of HA/0dECM and HA/10dECM, which contained a higher amount of HA, a larger proportion of HA was crosslinked when increasing the DVS ratio and this caused a greater decrease of the swelling ratio of these scaffolds. The highest swelling ratio of the HA/30dECM scaffold could be because of the swelling properties of collagen fibers presented in dECM.[44] A previous study on 3D gelatin/dECM-based
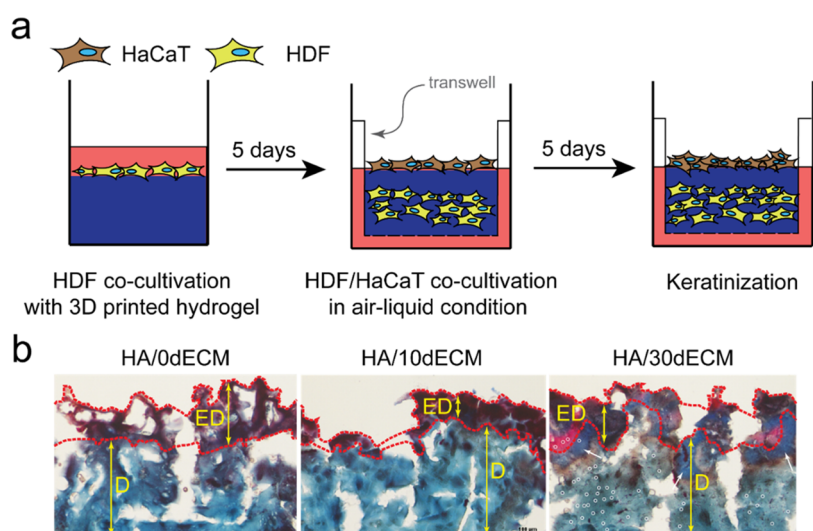
Figure 5. HDF and HaCaT cocultivation on 3D-printed scaffolds. (a) Cocultivation of the HDF/HaCaT/3D-printed model. After 5 d of incubation with HDF cells, HaCaT cells were added and incubated for another 5 days in air−liquid conditions to induce keratinization of HaCaT cells. (b) Masson's trichrome and hematoxylin staining of HDF and HaCaT-cocultivated 3D scaffolds. Collagens (white arrows) and cell nuclei (white circles) are stained in blue and violet. Dashed lines separate the regions of the epidermis (ED) and the dermis (D) (scale bar = 100 μm).

bioink reported that the 3D-printed model with the highest ratio of dECM showed the highest change in weight after incubation in the cell culture medium.[44] A DVS ratio of 7% (v/v) was used for further experiments to maintain suitable swelling properties for wound healing effects. Mass erosion of a crosslinked scaffold could be considered as a controllable factor for modulating the cell infiltration or drug release in different applications, and this property was influenced by the crosslinking degree.[42] After 7 d and up to 21 d of soaking in PBS, HA/0dECM exhibited the highest mass erosion among all other groups (Figure 3e). As aforementioned, 7% (v/v) of DVS would not be enough to fully crosslink the whole HA content in HA/0dECM and HA/10dECM. In addition, collagen fiber in dECM could enhance the mechanical property of the scaffold.[45] Thus, the 3D-printed model which contained the highest amount of the noncrosslinked HA and without dECM could be eroded more intensively than the dECM-contained scaffolds. HA/10dECM composed of the higher amount of crosslinked HA compared with HA/30dECM, which could result in lower mass erosion at day 21.

Cell viability analysis based on the WST-1 assay was performed to monitor NIH3T3 cell biocompatibility when seeding and culturing in a 3D circular model. According to the WST-1 assay (Figure 4), cell viability of HA/0dECM, HA/10dECM, and HA/30dECM increased 1.37, 1.23, and 1.46 times, respectively, when compared between day 3 and 7. The absorbance intensities of HA-based scaffolds containing fish-dECM were considerably higher than the ones without fish-dECM at any analyzed periods. Especially, when comparing the viability of NIH3T3 cells cultivated on HA/0dECM- and HA/30dECM-based printed models, there were notable differences of 1.88, 1.39, and 2 times on days 3, 5, and 7, respectively, which were supposed to be the effect of the solubilized decellularized fish-derived skin contained in the 3D circular model. In this research, the studied fish-dECM contained 35−40% collagen, 2.7−3.5% GAGs, and 2.0−2.5% growth factors (analyzed using a Sigma Aldrich hydroxyproline assay, Fastin elastin assay, and Blyscan sGAG assay, respectively); the presence of these components could enhance

cell proliferation, differentiation, and other cell functions, as reported in many previous studies.[46] Specifically, cell−ECM interactions supported by GAGs could further promote cell behaviors by direct interaction with cell membrane receptors and could serve as binding points for cells to recognize or adhere to the local ECM structure.[47,48] Therefore, higher cell viability and cell attachment (Figure 4a) was investigated in the 3D circular model containing a higher ratio of solubilized decellularized fish-derived skin in comparison with other groups.

To construct bilayered models mimicking human skin, HDF and HaCaT cells were cocultivated on the 3D models printed by HA/0dECM, HA/10dECM, and HA/30dECM bioinks (Figure 5a). Because of the risk of toxicity caused by DVS[49] and NaOH in a free form and the challenges in maintaining a clean environment for cell growth without any contamination during the whole 3D-printing process, cells were cultured on the 3D-printed scaffold instead of mixing with bioinks before printing process as this method has been used in numerous studies.[50,51] After 5 day-cultivation of HDF cells on the HA-based scaffolds to form the first dermal layer, HaCaT cells were subsequently seeded on top of the scaffolds and cultured in an air−liquid interface for another 5 days to induce keratinization. To observe the deposition of collagen and keratin in these cocultivated 3D models, Masson's trichrome and hematoxylin staining was applied on the 20 μm sections (Figure 5b). It was obviously seen that the collagen fibers, which were stained in blue, could be only noticed in the HA/30dECM-based scaffold among all groups. In addition, there was a large number of violet-stained cells infiltrating the dermis of the bilayer models fabricated from HA/30dECM bioink. In the other two scaffolds, violet-stained regions were observed in the epidermis, but not in the dermis; this could be due to the poor penetration of cells into the bilayered model. Previous studies reported that dECM could support cell interaction and attachment,[29,47,48] thereby suggesting that dECM would be crucial to attract HDF cells to be penetrated and distributed in the scaffold, and then involved in regulating collagen synthesis. Despite the presence of 10% of dECM, the HA/10dECM

scaffold did not show any different results compared to the biomodel without dECM. Thus, we supposed that the use of a sufficient amount of dECM should be critically considered to take advantage of dECM to enhance cell behaviors. In spite of the infiltration of fibroblasts into the 3D-printed scaffold, contraction was not observed, which could be because of the high mechanical properties of the scaffold owing to the presence of crosslinked HA.[52,53] Moreover, previous studies reported that embedded cells in the hydrogel during the gelling process could increase the tendency of the cells to contract the hydrogel, while spontaneous migration of the fibroblasts into the hydrogel could reduce the propensity of these cells to contract the scaffold by their traction forces.[54] Therefore, we speculated that our developed solubilized fish-dECM-combined HA-based 3D hybrid bioink can be potentially employed to construct a non-mammal-derived matrix for skin regeneration.

3. CONCLUSIONS

Fish-dECM was solubilized with alkaline conditions, and the soluble fraction of the solubilized dECM exhibited low cytotoxicity. Additionally, those with higher dECM contents showed better printability and injectability at higher concentrations of DVS when HA-based bioinks containing the solubilized dECM were printed into 3D hydrogels. Although various 3D-printed hydrogels were investigated with marginal differences in mass erosion rates and swelling ratios, dECM substantially enhanced the proliferation of cultivating cells for 7 days. Furthermore, bilayered skin models composed of epidermis and dermis were constructed with the 3D-printed hydrogels, and investigation by Masson's trichrome and hematoxyline staining indicated that the bio-scaffold with 30% solubilized fish-dECM could enhance cell infiltration into the dermis to induce collagen synthesis.

4. EXPERIMENTAL SECTION

4.1. Materials. Hyaluronic acid (1800−2500 kDa) was purchased from Stanford Chemicals (Lake Forest, CA). Decellularized fish-derived skin (fish-dECM) was provided by Innotherapy, Inc. (Seoul, Republic of Korea). Sodium hydroxide (NaOH) was purchased from Daejung Chemicals & Metals Co., Ltd. (Gyeonggi-do, Republic of Korea). Micro BCA Protein Assay Kit and human dermal fibroblast (HDF) were purchased from Thermo Fisher Scientific (Waltham, MA). Divinyl sulfone (DVS) was purchased from Alfa Aesar (Haverhill, MA). Dulbecco's modified Eagle's medium (DMEM), phosphate-buffered saline (PBS), and streptomycin/penicillin were purchased from Gibco (Grand Island, NY). Fetal bovine serum (FBS) was purchased from Corning (Corning, NY). Tissue-Tek OCT (optimal cutting temperature) compound was purchased from Sakura Finetek (Torrance, CA). Mouse embryonic fibroblast cell line NIH3T3 and human epidermal keratinocyte cell line HaCaT were obtained from the Korean Cell Line Bank (Seoul, Republic of Korea). The WST-1 (water-soluble tetrazolium salts) reagent (EZ Cytox) was purchased from DoGenBio Co., Ltd. (Seoul, Republic of Korea). Masson's trichrome and hematoxylin staining kit was purchased from VitroVivo Biotech (MD). All other chemicals were of analytical grade.

4.2. Preparation of Fish-dECM. The skin of *Seriola quinqueradiata* was polished by removing fish scales and flesh, followed by the decellularization in 0.5% Triton X-100 solution under stirring for 24 h. After that, the skin was washed using distilled water (DW) and then immersed in 5% hydrogen peroxide (H_2O_2) and 2% sodium metasilicate solution with continuous shaking for 2 h. The skin was subsequently washed using DW to remove the remaining chemicals and then freeze-dried. Cell cytotoxicity of the fish-dECM was evaluated by an indirect cytotoxicity test using the MTT assay. The cytotoxicity test was conducted following the ISO 10993-5 protocol. Fish-dECM was sterilized by ethylene oxide gas treatment and eluted using serum-contained media (6 cm^2 of fish-dECM in 1 mL of cell culture medium) at 37 °C for 24 h with gentle shaking. For the formation of the cell monolayer, 1 × 10⁴ of NIH3T3 cells were seeded on a 96-well plate and incubated at 37 °C for 24 h. The eluted medium was mixed with fresh serum-contained media at different mixing ratios (0−100%, v/v) and subsequently added to NIH3T3 cell monolayer (100 μL/ well) and then incubated at 37 °C for 24 h. After 24 h, an MTT-based cytotoxicity assay was performed, and the viability of the treated cells was normalized with respect to those without treatment.

4.3. Preparation of Solubilized Fish-dECM. For better dispersion in HA solution, fish-dECM was solubilized in an alkali condition. In particular, fish-dECM was cut into pieces (1 cm × 1 cm) and then 1 g of fish-dECM pieces (10%, w/v) were solubilized by immersing in 10 mL of 0.5 M NaOH solution at 25 °C for 12 h under magnetic stirring (Figure 1a). After 12 h, the mixture was centrifuged at 3000 rpm for 10 min to collect the solubilized fish-dECM in the supernatant and insolubilized fish-dECM was discarded. The remaining NaOH salt in the supernatant was removed via dialysis (molecular weight cutoff = 1000 Da) against DW at 25 °C for 48 h, followed by freeze-drying. The obtained solubilized fish-dECM powder was stored at −80 °C for further use. The solubilized fish-dECM was characterized by the BCA assay and UV spectroscopy. The BCA assay was performed following the recommended protocol from the manufacturer. In brief, the solubilized fish-dECM collected before and after dialysis was incubated with the BCA reagent at 37 °C for 1 h, and absorbance was measured at 562 nm using a plate reader (Multiskan GO; Thermo Scientific, U.K.). Bovine serum albumin (BSA) was used as the standard. UV−Vis spectra of the solubilized fish-dECM were recorded using a spectrophotometer (NanoVue Plus; GE Healthcare, U.K.) by scanning the wavelength from 200 to 400 nm.

4.4. Preparation of HA-Based Hybrid Ink. HA-based hybrid ink was prepared by mixing HA and solubilized fish-dECM. To prepare HA-based hybrid ink without solubilized fish-dECM (HA/0dECM), 1 g of HA was dissolved in 10 mL of 0.3 M NaOH solution at 25 °C for 24 h (Figure 1b). After that, DVS (6.2 μL; molar ratio of HA:DVS = 1:0.025) was added to the HA solution with magnetic stirring to prepare a pre-gel. To prepare 10 and 30% (w/w) fish-dECM hybrid ink (HA/10dECM, HA/30dECM), 1 g of HA was dissolved in 9 mL of 0.3 M NaOH solution at 25 °C for 24 h. Following that, 111.1 mg or 250 mg of the solubilized fish-dECM was dissolved in 1 mL of 0.3 M NaOH solution with respect to 10 or 30% of fish-dECM (prior to mixing with HA solution) by strong magnetic stirring for 30 min. DVS was added to HA/10dECM and HA/30dECM solution with a molar ratio of HA:DVS = 1:0.035 (8.8 μL) and 1:0.055 (13.8 μL), respectively. After 3 min of vigorous stirring, the HA/0dECM, HA/10dECM, and HA/30dECM solution was transferred to a 10 mL syringe and mild sonication (5510;

Branson, Danbury, CT) was applied for 2 min to remove the bubbles. The solution was further incubated at 25 °C for 1 h before 3D printing was performed.

4.5. 3D Printing. The 3D circular model was designed using Fusion 360 (Autodesk, CA). The designed model was saved as a standard triangle language (STL) file. The STL file was converted into G-code and the 3D circular model (diameter = 1.5 cm) was printed using a three-axis micro-positioning stage whose motions were controlled using New Creator K version 9.6.2 (ROKIT Healthcare, Republic of Korea). An extrude-based dispenser with a 0.4-mm nozzle and 10 mL syringe were used in this study. Extrusion conditions were set to a nozzle speed of 6 mm/s, an infill of 100%, and a layer height of 0.2 mm. The 3D circular model was printed on a dish. To optimize the condition, injectability and printability of the HA-based bioinks were evaluated based on the flowability of the bioinks and the shape fidelity of 3D-printed scaffolds within 1 min after printing. Low printability indicated the bioink, which formed a low undefined shape, mediate printability indicated the bioink with intermediate irregular patterns, and high printability indicated the bioink with a well-defined structure.[1] After printing, the DVS solution was prepared for the second crosslinking of the 3D model. Briefly, the crosslinking solution was prepared by mixing 12.5, 17.5, or 25 μL of DVS with 0.3 M sodium hydroxide solution to a final volume of 250 μL. The crosslinking solution was carefully dropped on the 3D circular model and incubated at 25 °C for 30 min. The 3D circular model was further washed three times with DW for 10 min to remove unreacted DVS and then freeze-dried and stored at −80°C for further uses.

4.6. Characterization of the 3D-Printed Model. The swelling ratio of the 3D-printed models was determined by measuring the weight of the 3D-printed models before and after swelling. The 3D-printed models were soaked in DW at 37 °C for 10, 30, 60, and 120 min, and then the excess water on the surface was carefully removed using Kimwipes for 20 s and the weight was measured. The swelling ratio of the 3D-printed models (n = 3) was gravimetrically determined using the following formula: swelling ratio (%) = (W_s/W_d) x 100 (%), where W_d is the dried weight of the 3D-printed model and W_s is the weight of the swollen 3D-printed model. The mass erosion of the 3D-printed models was determined by measuring the weight of the 3D-printed models before and after mass erosion. The 3D-printed models were soaked in phosphate-buffered saline (PBS) at 37 °C for 7, 14, and 21 days with orbital shaking (60 rpm). The supernatant was removed at designated time points and the 3D-printed models were washed five times with DW to remove residual salt and then freeze-dried.

4.7. *In Vitro* Cell Cultivation. HA/0dECM, HA/10dECM, or HA/30dECM printed models were sterilized by immersing in 70% (v/v) ethanol and irradiating under UV light for 1 h. The sterilized samples were transferred to a nontreated 12-well plate and washed five times with 1 mL of cell culture medium for 10 min each. A suspension of NIH3T3 cells (0.5 mL, 2×10^5 cells/well) in DMEM supplemented with 10% (v/v) FBS and 1% (v/v) streptomycin/penicillin was seeded on each well. After that, the cell-seeded 3D samples were cultured at 37 °C under 5% CO_2 for 12 h and 0.5 mL of the cell culture medium was added to each well (final volume = 1 mL/well). After 1 day of incubation, the cell-seeded 3D samples were carefully washed three times with PBS to remove unattached cells, and these unattached cells were collected for trypan blue

staining and counted using a hemocytometer. The cell attachment (%) was determined by measuring the initial number of seeded cells and the unattached cells.

To evaluate cell proliferation, the cell-seeded 3D samples were incubated at 37 °C under 5% CO_2 for 3, 5, and 7 days. After each mentioned specific period, the cell proliferation was determined using a WST-1-based colorimetric assay according to the protocol of the manufacturer. Briefly, the entire medium in the nontreated 12-well plate was discarded, and 1 mL of fresh medium was added. After that, 0.1 mL of WST-1 reagent was added to each well and incubated at 37 °C under 5% CO_2 for 1 h. The absorbance of the medium was measured at 450 nm using a plate reader (Multiskan GO; Thermo Scientific, U.K.).

4.8. *In Vitro* Construction of Bilayered Human Skin. HA/0dECM, HA/10dECM, or HA/30dECM printed scaffolds cut into 0.5 cm × 0.5 cm were sterilized by immersing in 70% (v/v) ethanol and irradiating under UV light for 1 h. The sterilized samples were washed five times with 1 mL of cell culture medium for 10 min each, and transferred to a nontreated 96-well plate. A suspension of HDF cells (0.02 mL, 5×10^4 cells/well) in DMEM supplemented with low serum growth supplement (LSGS) and streptomycin/penicillin was seeded on each well, and 0.03 mL of the cell culture medium was subsequently added. After that, the cell-seeded 3D samples were cultured at 37 °C under 5% CO_2. The cell culture medium was replaced daily with fresh medium. After 5 d of incubation, the HDF-seeded 3D samples were transferred to a transwell (24-well plate with insert), and a suspension of HaCaT cells (0.02 mL, 5×10^4 cells/well) in DMEM supplemented with 10% (v/v) FBS and 1% (v/v) streptomycin/ penicillin was seeded on each well (final volume = 0.4 mL). For keratinization, HDF and HaCaT cell-seeded 3D model was cultured in an air−liquid environment for 5 d.

The cocultivated 3D models were fixed with 2.5% (v/v) glutaraldehyde in PBS (pH 7.4) at 4 °C overnight. The fixed 3D scaffolds were washed three times with PBS, dehydrated in 30% sucrose solution, and embedded in Tissue-Tek OCT compound. The samples were sectioned into 20 μm-thick slices using a cryostat microtome (CM1850; Leica, Deer Park, IL), and stained with Masson's trichrome staining reagents following the protocol of the manufacturer to observe the deposition of collagen and keratin. Briefly, 3D model sections were immersed in DW for 3 min to remove the O.C.T compound and then mordanted in Bouin's solution for 1 h at 60 °C, followed by washing under running tap water for 5 min. The 3D model sections were stained with Weigert's hematoxylin for 10 min and washed under running tap water for 5 min before being incubated in scarlet acid fuchsin solution for 5 min at 25 ± 2 °C, and washed in DW for 1 min. These sections were treated with phosphotungstic acid solution for 10 min at 25 ± 2 °C, and counter-stained with Aniline Blue for another 10 min, followed by differentiation in 1% acetic acid in DW for 1 min. The stained 3D model sections were subsequently washed with DW, dehydrated in gradient concentrations of ethanol, and cleared using xylene. The dehydrated 3D model sections were mounted using nail polish for visualization under a fluorescence microscope (Eclipse Ti-S; Nikon, Japan).

4.9. Statistical Analysis. Statistical analysis was performed using a one-way ANOVA in the SigmaPlot 14.0 software, and p-values < 0.05 were considered statistically significant.

■ ASSOCIATED CONTENT

Ⓢ Supporting Information

The Supporting Information is available free of charge at https://pubs.acs.org/doi/10.1021/acsomega.3c01642.

UV−vis spectra of solubilized fish-dECM before or after dialysis (Figure S1) and the water swelling ratio of 3D-printed models with 5 and 10% DVS (Figure S2) (PDF)

■ AUTHOR INFORMATION

Corresponding Author

Hyuk Sang Yoo − *Department of Medical Biomaterials Engineering, Kangwon National University, Chuncheon 24341, Republic of Korea; Kangwon Radiation Convergence Research Support Center, Institute of Bioscience & Biotechnology, and Institute of Molecular Science and Fusion Technology, Kangwon National University, Chuncheon 24341, Republic of Korea;* ⓘ orcid.org/0000-0002-4346-9154; Email: hsyoo@kangwon.ac.kr

Authors

Hoai-Thuong Duc Bui − *Department of Medical Biomaterials Engineering, Kangwon National University, Chuncheon 24341, Republic of Korea*

Wanho Cho − *Department of Medical Biomaterials Engineering, Kangwon National University, Chuncheon 24341, Republic of Korea*

Jae Keun Park − *Department of Medical Biomaterials Engineering, Kangwon National University, Chuncheon 24341, Republic of Korea*

Moon Sue Lee − *R&D center, InnoTherapy Inc., Seoul 07282, Republic of Korea*

Hong Kee Kim − *R&D center, InnoTherapy Inc., Seoul 07282, Republic of Korea*

Complete contact information is available at:
https://pubs.acs.org/10.1021/acsomega.3c01642

Author Contributions

H.-T.D.B., W.C., and J.K.P.: methodology, investigation, and writing—original draft preparation; M.S.L. and H.K.K.: funding acquisition and supervision; H.S.Y.: writing the original manuscript, validation, writing—review and editing, and funding acquisition

Funding

Notes

The authors declare no competing financial interest.

■ REFERENCES

(1) Kiyotake, E. A.; Douglas, A. W.; Thomas, E. E.; Nimmo, S. L.; Detamore, M. S. Development and Quantitative Characterization of the Precursor Rheology of Hyaluronic Acid Hydrogels for Bioprinting. *Acta Biomater.* 2019, 95, 176−187.

(2) Ge, B.; Wang, H.; Li, J.; Liu, H.; Yin, Y.; Zhang, N.; Qin, S. Comprehensive Assessment of Nile Tilapia Skin. *Mar. Drugs* 2021, 18, 178−194.

(3) Ouyang, L.; Highley, C. B.; Rodell, C. B.; Sun, W.; Burdick, J. A. 3D Printing of Shear-Thinning Hyaluronic Acid Hydrogels with Secondary Cross-Linking. *ACS Biomater. Sci. Eng.* 2016, 2, 1743−1751.

(4) Petta, D.; Armiento, A. R.; Grijpma, D.; Alini, M.; Eglin, D.; D'Este, M. 3D Bioprinting of a Hyaluronan Bioink through Enzymatic-and Visible Light-Crosslinking. *Biofabrication* 2018, 10, No. 044104.

(5) Petta, D.; D'Amora, U.; Ambrosio, L.; Grijpma, D. W.; Eglin, D.; D'Este, M. Hyaluronic Acid as a Bioink for Extrusion-Based 3D Printing. *Biofabrication* 2020, 12, No. 032001.

(6) Qiao, Y.; Xu, S.; Zhu, T.; Tang, N.; Bai, X.; Zheng, C. Preparation of Printable Double-Network Hydrogels with Rapid Self-Healing and High Elasticity Based on Hyaluronic Acid for Controlled Drug Release. *Polymer* 2020, 186, No. 121994.

(7) Antich, C.; de Vicente, J.; Jiménez, G.; Chocarro, C.; Carrillo, E.; Montañez, E.; Gálvez-Martín, P.; Marchal, J. A. Bio-Inspired Hydrogel Composed of Hyaluronic Acid and Alginate as a Potential Bioink for 3D Bioprinting of Articular Cartilage Engineering Constructs. *Acta Biomater.* 2020, 106, 114−123.

(8) Roushangar Zineh, B.; Shabgard, M. R.; Roshangar, L.; Jahani, K. Experimental and Numerical Study on the Performance of Printed Alginate/Hyaluronic Acid/Halloysite Nanotube/Polyvinylidene Fluoride Bio-Scaffolds. *J. Biomech.* 2020, 104, No. 109764.

(9) Pérez, L. A.; Hernández, R.; Alonso, J. M.; Pérez-González, R.; Sáez-Martínez, V. Hyaluronic Acid Hydrogels Crosslinked in Physiological Conditions: Synthesis and Biomedical Applications. *Biomedicines* 2021, 9, No. 1113.

(10) Yang, R.; Tan, L.; Cen, L.; Zhang, Z. An Injectable Scaffold Based on Crosslinked Hyaluronic Acid Gel for Tissue Regeneration. *RSC Adv.* 2016, 6, 16838−16850.

(11) Collins, M. N.; Birkinshaw, C. Hyaluronic Acid Based Scaffolds for Tissue Engineering - A Review. *Carbohydr. Polym.* 2013, 92, 1262−1279.

(12) Khunmanee, S.; Jeong, Y.; Park, H. Crosslinking Method of Hyaluronic-Based Hydrogel for Biomedical Applications. *J. Tissue Eng.* 2017, 8, No. 204173141772646.

(13) Seif-Naraghi, S. B.; Horn, D.; Schup-Magoffin, P. J.; Christman, K. L. Injectable Extracellular Matrix Derived Hydrogel Provides a Platform for Enhanced Retention and Delivery of a Heparin-Binding Growth Factor. *Acta Biomater.* 2012, 8, 3695−3703.

(14) Seo, Y.; Jung, Y.; Kim, S. H. Decellularized Heart ECM Hydrogel Using Supercritical Carbon Dioxide for Improved Angiogenesis. *Acta Biomater.* 2018, 67, 270−281.

(15) Bordbar, S.; Bakhshaiesh, N. L.; Khanmohammadi, M.; Sayahpour, F. A.; Alini, M.; Baghaban Eslaminejad, M. Production and Evaluation of Decellularized Extracellular Matrix Hydrogel for Cartilage Regeneration Derived from Knee Cartilage. *J. Biomed. Mater. Res., Part A* 2020, 108, 938−946.

(16) Wolf, M. T.; Daly, K. A.; Brennan-Pierce, E. P.; Johnson, S. A.; Carruthers, C. A.; D'Amore, A.; Nagarkar, S. P.; Velankar, S. S.; Badylak, S. F. A Hydrogel Derived from Decellularized Dermal Extracellular Matrix. *Biomaterials* 2012, 33, 7028−7038.

(17) Badylak, S. F.; Freytes, D. O.; Gilbert, T. W. Extracellular Matrix as a Biological Scaffold Material: Structure and Function. *Acta Biomater.* 2009, 5, 1−13.

(18) Xu, J.; Fang, H.; Zheng, S.; Li, L.; Jiao, Z.; Wang, H.; Nie, Y.; Liu, T.; Song, K. A Biological Functional Hybrid Scaffold Based on Decellularized Extracellular Matrix/Gelatin/Chitosan with High Biocompatibility and Antibacterial Activity for Skin Tissue Engineering. *Int. J. Biol. Macromol.* 2021, 187, 840−849.

(19) Su, Z.; Ma, H.; Wu, Z.; Zeng, H.; Li, Z.; Wang, Y.; Liu, G.; Xu, B.; Lin, Y.; Zhang, P.; Wei, X. Enhancement of Skin Wound Healing with Decellularized Scaffolds Loaded with Hyaluronic Acid and Epidermal Growth Factor. *Mater. Sci. Eng. C* 2014, 44, 440−448.

(20) Chen, W.; Xu, Y.; Li, Y.; Jia, L.; Mo, X.; Jiang, G.; Zhou, G. 3D Printing Electrospinning Fiber-Reinforced Decellularized Extracellular Matrix for Cartilage Regeneration. *Chem. Eng. J.* 2020, 382, No. 122986.

(21) Wang, Z.; Li, Z.; Li, Z.; Wu, B.; Liu, Y.; Wu, W. Cartilaginous Extracellular Matrix Derived from Decellularized Chondrocyte Sheets for the Reconstruction of Osteochondral Defects in Rabbits. *Acta Biomater.* 2018, 81, 129−145.

(22) Han, T. T. Y.; Toutounji, S.; Amsden, B. G.; Flynn, L. E. Adipose-Derived Stromal Cells Mediate in Vivo Adipogenesis, Angiogenesis and Inflammation in Decellularized Adipose Tissue Bioscaffolds. *Biomaterials* **2015**, *72*, 125−137.

(23) Han, W.; Singh, N. K.; Kim, J. J.; Kim, H.; Kim, B. S.; Park, J. Y.; Jang, J.; Cho, D. W. Directed Differential Behaviors of Multipotent Adult Stem Cells from Decellularized Tissue/Organ Extracellular Matrix Bioinks. *Biomaterials* **2019**, *224*, No. 119496.

(24) Zhou, H.; Chen, R.; Wang, J.; Lu, J.; Yu, T.; Wu, X.; Xu, S.; Li, Z.; Jie, C.; Cao, R.; Yang, Y.; Li, Y.; Meng, D. Biphasic Fish Collagen Scaffold for Osteochondral Regeneration. *Mater. Des.* **2020**, *195*, No. 108947.

(25) Kirsner, R. S.; Margolis, D. J.; Baldursson, B. T.; Petursdottir, K.; Davidsson, O. B.; Weir, D.; Lantis, J. C. Fish Skin Grafts Compared to Human Amnion/Chorion Membrane Allografts: A Double-Blind, Prospective, Randomized Clinical Trial of Acute Wound Healing. *Wound Repair Regener.* **2020**, *28*, 75−80.

(26) Govindharaj, M.; Roopavath, U. K.; Rath, S. N. Valorization of Discarded Marine Eel Fish Skin for Collagen Extraction as a 3D Printable Blue Biomaterial for Tissue Engineering. *J. Cleaner Prod.* **2019**, *230*, 412−419.

(27) Blanco, M.; Vázquez, J. A.; Pérez-Martín, R. I.; Sotelo, C. G. Collagen Extraction Optimization from the Skin of the Small-Spotted Catshark (S. Canicula) by Response Surface Methodology. *Mar. Drugs* **2019**, *17*, No. 40.

(28) Lim, Y.; Ok, Y.-J.; Hwang, S.; Kwak, J.; Yoon, S. Marine Collagen as A Promising Biomaterial For. *Mar. Drugs* **2019**, *17*, No. 467.

(29) Girardeau-Hubert, S.; Lynch, B.; Zuttion, F.; Label, R.; Rayee, C.; Brizion, S.; Ricois, S.; Martinez, A.; Park, E.; Kim, C.; Marinho, P. A.; Shim, J. H.; Jin, S.; Rielland, M.; Soeur, J. Impact of Microstructure on Cell Behavior and Tissue Mechanics in Collagen and Dermal Decellularized Extra-Cellular Matrices. *Acta Biomater.* **2022**, *143*, 100−114.

(30) Chameettachal, S.; Sasikumar, S.; Sethi, S.; Sriya, Y.; Pati, F. Tissue/Organ-Derived Bioink Formulation for 3D Bioprinting. *J. 3D Print. Med.* **2019**, *3*, 39−54.

(31) Reing, J. E.; Brown, B. N.; Daly, K. A.; Freund, J. M.; Gilbert, T. W.; Hsiong, S. X.; Huber, A.; Kullas, K. E.; Tottey, S.; Wolf, M. T.; Badylak, S. F. The Effects of Processing Methods upon Mechanical and Biologic Properties of Porcine Dermal Extracellular Matrix Scaffolds. *Biomaterials* **2010**, *31*, 8626−8633.

(32) Zhang, Q.; Johnson, J. A.; Dunne, L. W.; Chen, Y.; Iyyanki, T.; Wu, Y.; Chang, E. I.; Branch-Brooks, C. D.; Robb, G. L.; Butler, C. E. Decellularized Skin/Adipose Tissue Flap Matrix for Engineering Vascularized Composite Soft Tissue Flaps. *Acta Biomater.* **2016**, *35*, 166−184.

(33) Liu, D.; Wei, G.; Li, T.; Hu, J.; Lu, N.; Regenstein, J. M.; Zhou, P. Effects of Alkaline Pretreatments and Acid Extraction Conditions on the Acid-Soluble Collagen from Grass Carp (Ctenopharyngodon Idella) Skin. *Food Chem.* **2015**, *172*, 836−843.

(34) Meng, D.; Tanaka, H.; Kobayashi, T.; Hatayama, H.; Zhang, X.; Ura, K.; Yunoki, S.; Takagi, Y. The Effect of Alkaline Pretreatment on the Biochemical Characteristics and Fibril-Forming Abilities of Types I and II Collagen Extracted from Bester Sturgeon by-Products. *Int. J. Biol. Macromol.* **2019**, *131*, 572−580.

(35) Furtado, M.; Chen, L.; Chen, Z.; Chen, A.; Cui, W. Development of Fish Collagen in Tissue Regeneration and Drug Delivery. *Eng. Regen.* **2022**, *3*, 217−231.

(36) Yoshimura, K.; Terashima, M.; Hozan, D.; Shirai, K. Preparation and Dynamic Viscoelasticity Characterization of Alkali-Solubilized Collagen from Shark Skin. *J. Agric. Food Chem.* **2000**, *48*, 685−690.

(37) Bowes, J. H.; Kenten, R. H. The Effect of Alkalis on Collagen. *Biochem. J.* **1948**, *43*, 365−372.

(38) Hattori, S.; Adachi, E.; Ebihara, T.; Shirai, T.; Someki, I.; Irie, S. Alkali-Treated the Ligand Collagen Activity Retained the the Adhesion Triple via Conformation Integrin for The Method of Extracting Collagen from Connective Tissue with a Solution of Sodium Hydroxide and Monomethylamine Was Developed about 30 Years Ago (. *J. Biochem.* **1999**, *125*, 676−684.

(39) Yan, M.; Li, B.; Zhao, X.; Ren, G.; Zhuang, Y.; Hou, H.; Zhang, X.; Chen, L.; Fan, Y. Characterization of Acid-Soluble Collagen from the Skin of Walleye Pollock (Theragra Chalcogramma). *Food Chem.* **2008**, *107*, 1581−1586.

(40) Nurubhasha, R.; Kumar, N. S. S.; Thirumalasetti, S. K.; Simhachalam, G.; Dirisala, V. R. Extraction and Characterization of Collagen from the Skin of Pterygoplichthys Pardalis and Its Potential Application in Food Industries. *Food Sci. Biotechnol.* **2019**, *28*, 1811−1817.

(41) Kamalvand, M.; Biazar, E.; Daliri-Joupari, M.; Montazer, F.; Rezaei-Tavirani, M.; Heidari-Keshel, S. Design of a Decellularized Fish Skin as a Biological Scaffold for Skin Tissue Regeneration. *Tissue Cell* **2021**, *71*, No. 101509.

(42) Lu, H. D.; Soranno, D. E.; Rodell, C. B.; Kim, I. L.; Burdick, J. A. Secondary Photocrosslinking of Injectable Shear-Thinning Dock-and-Lock Hydrogels. *Adv. Healthcare Mater.* **2013**, *2*, 1028−1036.

(43) Guo, S.; DiPietro, L. A. Critical Review in Oral Biology & Medicine: Factors Affecting Wound Healing. *J. Dent. Res.* **2010**, *89*, 219−229.

(44) Kara, A.; Distler, T.; Polley, C.; Schneidereit, D.; Seitz, H.; Friedrich, O.; Tihminlioglu, F.; Boccaccini, A. R. 3D Printed Gelatin/Decellularized Bone Composite Scaffolds for Bone Tissue Engineering: Fabrication, Characterization and Cytocompatibility Study. *Mater. Today Bio* **2022**, *15*, No. 100309.

(45) Shirazi, R.; Shirazi-Adl, A.; Hurtig, M. Role of Cartilage Collagen Fibrils Networks in Knee Joint Biomechanics under Compression. *J. Biomech.* **2008**, *41*, 3340−3348.

(46) Ying, H.; Zhou, J.; Wang, M.; Su, D.; Ma, Q.; Lv, G.; Chen, J. In Situ Formed Collagen-Hyaluronic Acid Hydrogel as Biomimetic Dressing for Promoting Spontaneous Wound Healing. *Mater. Sci. Eng. C* **2019**, *101*, 487−498.

(47) Uhl, F. E.; Zhang, F.; Pouliot, R. A.; Uriarte, J. J.; Rolandsson Enes, S.; Han, X.; Ouyang, Y.; Xia, K.; Westergren-Thorsson, G.; Malmström, A.; Hallgren, O.; Linhardt, R. J.; Weiss, D. J. Functional Role of Glycosaminoglycans in Decellularized Lung Extracellular Matrix. *Acta Biomater.* **2020**, *102*, 231−246.

(48) Linhardt, R. J.; Toida, T. Linhardt.ReviewGAG.121130.Pdf. *Acc. Chem. Res.* **2004**, *37*, 431−438.

(49) West, J. D.; West, J. D.; Stamm, C. E.; Brown, H. A.; Justice, S. L.; Morano, K. A. Enhanced Toxicity of the Protein Cross-Linkers Divinyl Sulfone and Diethyl Acetylenedicarboxylate in Comparison to Related Monofunctional Electrophiles. *Chem. Res. Toxicol.* **2011**, *24*, 1457−1459.

(50) Fang, Y.; Han, Y.; Wang, S.; Chen, J.; Dai, K.; Xiong, Y.; Sun, B. Three-Dimensional Printing Bilayer Membranous Nanofiber Scaffold for Inhibiting Scar Hyperplasia of Skin. *Biomater. Adv.* **2022**, *138*, No. 212951.

(51) Zhang, T.; Xu, H.; Zhang, Y.; Zhang, S.; Yang, X.; Wei, Y.; Huang, D.; Lian, X. Fabrication and Characterization of Double-Layer Asymmetric Dressing through Electrostatic Spinning and 3D Printing for Skin Wound Repair. *Mater. Des.* **2022**, *218*, No. 110711.

(52) Randall, M. J.; Jüngel, A.; Rimann, M.; Wuertz-Kozak, K. Advances in the Biofabrication of 3D Skin in Vitro: Healthy and Pathological Models. *Front. Bioeng. Biotechnol.* **2018**, *6*, No. 154.

(53) Kim, S.; Lee, H.; Kim, J. A.; Park, T. H. Prevention of Collagen Hydrogel Contraction Using Polydopamine-Coating and Alginate Outer Shell Increases Cell Contractile Force. *Biomater. Adv.* **2022**, *136*, No. 212780.

(54) Bacakova, M.; Pajorova, J.; Broz, A.; Hadraba, D.; Lopot, F.; Zavadakova, A.; Vistejnova, L.; Kostic, I.; Jencova, V.; Bacakova, L. Erratum to a Two-Layer Skin Construct Consisting of a Collagen Hydrogel Reinforced by a Fibrin-Coated Polylactide Nanofibrous Membrane (Int J Nanomedicine, (2019), 14, (5033−5050)). *Int. J. Nanomed.* **2019**, *14*, 7215−7216.